ICIS
EUROPEAN INTERNET CENTRE FOR IMPEDANCE SPECTROSCOPY
***Impedance Contributions Online* 9 (2011) P3-1 – P3-14**
http://accessimpedance.iusi.bas.bg

THE INTEGRATION OF EIS PARAMETERS AND BULK MATRIX CHARACTERISTICS IN STUDYING REINFORCED CEMENT-BASED MATERIALS

D.A. Koleva*, K. van Breugel

Delft University of Technology, Faculty of Civil Engineering & Geosciences, Department Materials & Environment, Stevinweg 1, 2628 CN, Delft, The Netherlands
**Corresponding author: D.A.Koleva@tudelft.nl*

ABSTRACT

Corrosion in reinforced concrete is a major and costly concern, arising from the higher complexity of involved phenomena on different levels of material science (e.g. electrochemistry, concrete material science) and material properties (macro/micro/ nano). Reinforced cement-based systems (e.g. reinforced mortar and concrete) are multi-phase composite materials at different levels of aggregation. Hence, multi-phase interfaces are involved in their structural performance and material behavior. Reinforced concrete has the potential to be durable and capable of withstanding a variety of adverse environmental conditions. One of the major difficulties in the engineering practice, however, is the multi-dimensional nature of reinforcement corrosion related issues. Nevertheless, materials and processes involved in the service life of a civil structure and their interaction are independently weighed and are seldom brought together. Very often the design of concrete mix proportions and the design of protective measures (such as the application of coatings or electrochemical techniques) are made in separate steps and (positive or negative) interactions among themselves are neglected.

This work reports on the integration of fundamental electrochemical techniques (as Electrochemical impedance spectroscopy) and concrete material science (bulk matrix properties) within monitoring and assessment of the corrosion performance of reinforced cement-based materials. Further, hereby discussed is the implementation of an eco-friendly approach of waste utilization for corrosion control and/or achieving superior properties and performance.

Key words: Reinforced concrete; Corrosion; EIS; Microstructure; Red mud

1. INTRODUCTION

The main objective of this study is to illustrate the synergy of electrochemistry (in terms of steel corrosion resistance) and concrete material science (mainly in terms of evaluation concrete bulk matrix properties) in studying reinforced cement-based systems. The paper briefly presents part of a comparative investigation of the corrosion behavior of reinforcing steel in concrete, using Ordinary Portland cement (OPC), Blast furnace slag cement (BFS) and Red Mud (RM) in chloride containing environment. The variables of main interest are: the corrosion parameters of the steel reinforcement and the alterations in the bulk cement-based matrix (porosity, pore size distribution). The investigation is performed as a comparative study of control (non-corroding) specimens from each group and corroding such (conditioned in 5% NaCl).

Steel corrosion, being a major problem in civil engineering, presents a huge cost (e.g. 30 to 50% of annual costs for infrastructure maintenance in EU are spent on corrosion-related issues). Dealing with steel corrosion in an eco-friendly manner, using wastes for example, is a sustainable way of solving corrosion problems. Additionally, the cement replacement by wastes in a reinforced concrete system would even further create sustainable solutions (less cement utilization, less CO_2 produced).

Recycling of waste materials in the construction industry is an eco-friendly and a technically successful option. However, major wastes (e.g. the bauxite residue – the highly alkaline red mud) are still not practically utilized and cause serious and alarming environmental issues: each tone of produced aluminum results in 0.5–2 tones waste; approximately 145 million tones of red mud are annually produced [1]. Red mud (RM) is reported to increase steel passivity in alkaline solutions [2]; RM additions to cement-based materials are also recently reported to result in mortars and concretes for shielding X-ray radiation [3], heavy metal (and other toxic substances) binding effects [4-6] while maintaining sufficient mechanical properties [7]. Practical applications are however extremely limited.

Blast furnace slag (BFS) is another largely generated waste (from the steel production); in contrast to RM, it is widely used in European countries; e.g. in The Netherlands it has a market share of more than 50%. A practical inconvenience however is the impeded cement hydration of BFS, compared to Portland cement

(OPC) [8,9], resulting in a coarser structure at earlier hydration ages. Further, BFS concrete requires proper and careful water curing at early ages and even then, reinforcing steel in BFS concrete exhibits reduced properties of the passive layer, due to: limited oxygen availability and thus a shift of the steel corrosion potential to a more negative state [10,11]; lower calcium content and pH decrease [12]. Despite the higher chloride binding capacity of BFS, the passive layer on the steel surface is weakened as the Fe^{3+} species are reduced by the reducing agents from BFS cement itself; additionally BFS concrete is highly susceptible to carbonation and freeze-thaw durability issues [13].

To this end, the present contribution reports on the investigation of both BFS and RM containing reinforced mortar. Further, a mixture of RM and BFS as OPC cement replacement was also studied. A comparative investigation of control and corroding cells is presented for the period of approximately 250 days of conditioning (the test is still on-going).

2. EXPERIMENTAL

2.1. Materials

Reinforced mortar cylinders (d = 3.5 cm; h = 20cm) were cast from OPC CEM I 42.5 and CEM IIIB 42.5, cement/sand ratio of 1:3 and water/cement ratio of 0.6. The waste Red mud (RM) was added as 20% OPC or BFS replacement (chemical composition in Table 1). Eight groups (5 replicates per group) were monitored: four control groups (non-corroding) with (designation RM) and without red mud, denoted as OPC, RMOPC, BFS and RMBFS respectively, and four corroding groups, with and without red mud, denoted OPCn, RMOPCn, BFSn and RMBFSn. All specimens were cured for 7 days in fog room (20 ºC and 98% RH) and maintained in lab air further on. An external solution of 10 % NaCl was used as a chloride-induced accelerator for the corroding groups (the specimens were 1/3rd of height immersed in the solution; the control specimens were immersed in tap water). Red mud was added (after drying at 105ºC and grinding to cement finesse) for the RMOPC, RMOPCn, RMBFS and RMBFSn specimens.

Table 1. Chemical composition, main compounds (dry cements (ENCI. NL) and red mud, as received)

Wt. %	OPC (CEM I) (ENCI, NL)	BFS (CEM III B) (ENCI, NL)	RM (XRF)
CaO	61.0	48.0	3.5
SiO_2	19.0	29.0	20.2
Na_2O	Alkali	Alkali	14.3
K_2O	Equivalent: 1.12	Equivalent: 0.9	0.1
Al_2O_3	4.90	9.70	29.1
Fe_2O_3	3.50	1.48	24.9
MgO	1.80	5.20	0.1
SO_3	3.50	2.70	0.5
Cl	0.09	0.05	0.14

The chemical and mineralogical composition of red mud depends on the processed bauxite, the aluminum production process itself and the geographical location. The red mud used in this study was supplied from Suriname (XRF analysis of the received supply gives major contributions of: Al_2O_3 29.1 wt.%, Fe_2O_3 24.9 wt.%, Na_2O 14.3 wt.%, SiO_2 20.2 wt.%, CaO 3.5 wt.%). The steel re-bars (construction steel FeB500 HKN, d=0.8cm, h=10cm, exposed surface of 21 cm^2, composition according NEN6008 (in wt.%): C < 0.12 wt.%, Si max 0.6, P max 0.05, S max 0.05, N max 0.012) were embedded “as received” i.e. there was no preliminary treatment of the bars before casting. Both ends of the steel bars were isolated (to avoid crevice corrosion) and the bar was positioned in the middle of the concrete specimens. Mixed Metal Oxide (MMO) titanium mesh served as a counter electrode; SCE electrode was used as a reference electrode. The experimental set-up and specimen’s geometry are as previously used and reported in [14,15].

2.2. Methods

With regard to the experimental results and discussion, which this paper briefly summarizes, the following methods and techniques are relevant.

- Scanning electron microscopy, coupled with EDX analysis (using ESEM Philips XL30);
- Open circuit potential (OCP), Electrochemical Impedance Spectroscopy (EIS) and Potentio-dynamic polarization (PDP), using EcoChemie Autolab.
- Microstructure and image analysis (for porosity and pore size distribution) ESEM for imaging and visualization of morphological and microstructure investigation; OPTIMAS software was used for image analysis (for image analysis, a set of ESEM

images of the cement matrix was obtained in backscattered electron (BSE) mode with the magnification of 500x. The results are an average of 35 locations per sample (details about the sample preparation and procedures as reported in [16-20]).

3. RESULTS AND DISCUSSION

3.1. Electrochemical Impedance Spectroscopy (EIS)

EIS is a useful technique for obtaining knowledge of the steel/concrete system as it provides information for both the steel surface (electrochemical parameters) and the concrete bulk matrix (concrete bulk and pore network resistance) [21,22]. Figure 1 depicts the equivalent electrical circuit, used for interpretation and data fitting of the experimental EIS response (the circuit is based on previously used and reported such for reinforced cement-based systems [14,23], including additional parameters to account for bulk matrix properties [24], considering the frequency range hereby used of 1MHz to 10mHz.

The elements of the equivalent circuit present the following physical meaning: The first part of the circuit i.e. the high frequency domain (C1,R1 and C2, R2) is attributed to the properties of the concrete matrix in terms of pore network: solid phase and disconnected pore pathways and the resistance of the pore network in terms of continuous connected pores; The second part of the circuit i.e. middle and low frequency domains (time constants R3C3 and R4C4) deals with the electrochemical reaction on the steel surface including the contribution of redox processes, taking place in the product layers on the steel surface. An overlay of the experimental EIS response for all groups is presented in Fig.2 relevant to the final so far recorded time interval of 250 days, which corresponds to the time interval of microstructural analysis. Summarized data for the best fit parameters are presented in Table 2.

The high frequency response corresponds to the concrete bulk resistance, including the contribution of electrolyte resistance (electrolyte resistance was in the range of 10 ohm for corroding cases to 30 for control cases). For deriving polarization resistance (R_p) from EIS measurements in reinforced concrete (R_{ct} and R_{red} respectively), the medium-low and low frequency limits of the impedance spectra are generally considered, as reported in [25-28], previously discussed and

reported for reinforced mortar and concrete in [14,23] and used in the present study as well.

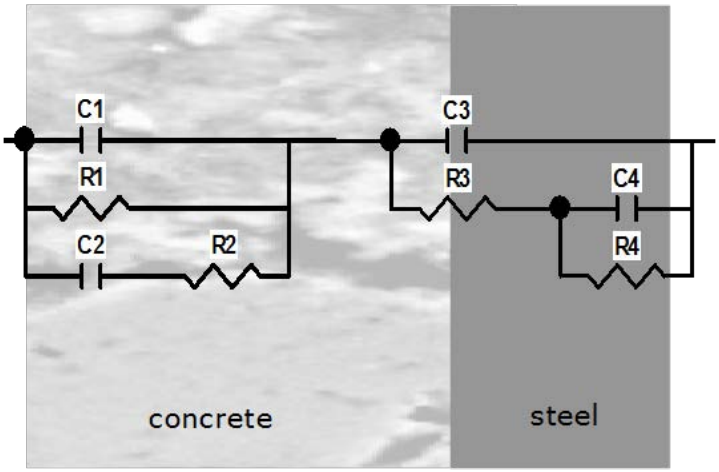

Fig.1 Equivalent electrical circuit: C1R1 = capacitance and resistance of disconnected pore pathways incl. solid phase; C2R2 = capacitance and resistance of pore network (continuous conductive paths); C3R3 = charge transfer resistance and double layer capacitance (steel reinforcement); C4R4 = product layer characteristics.

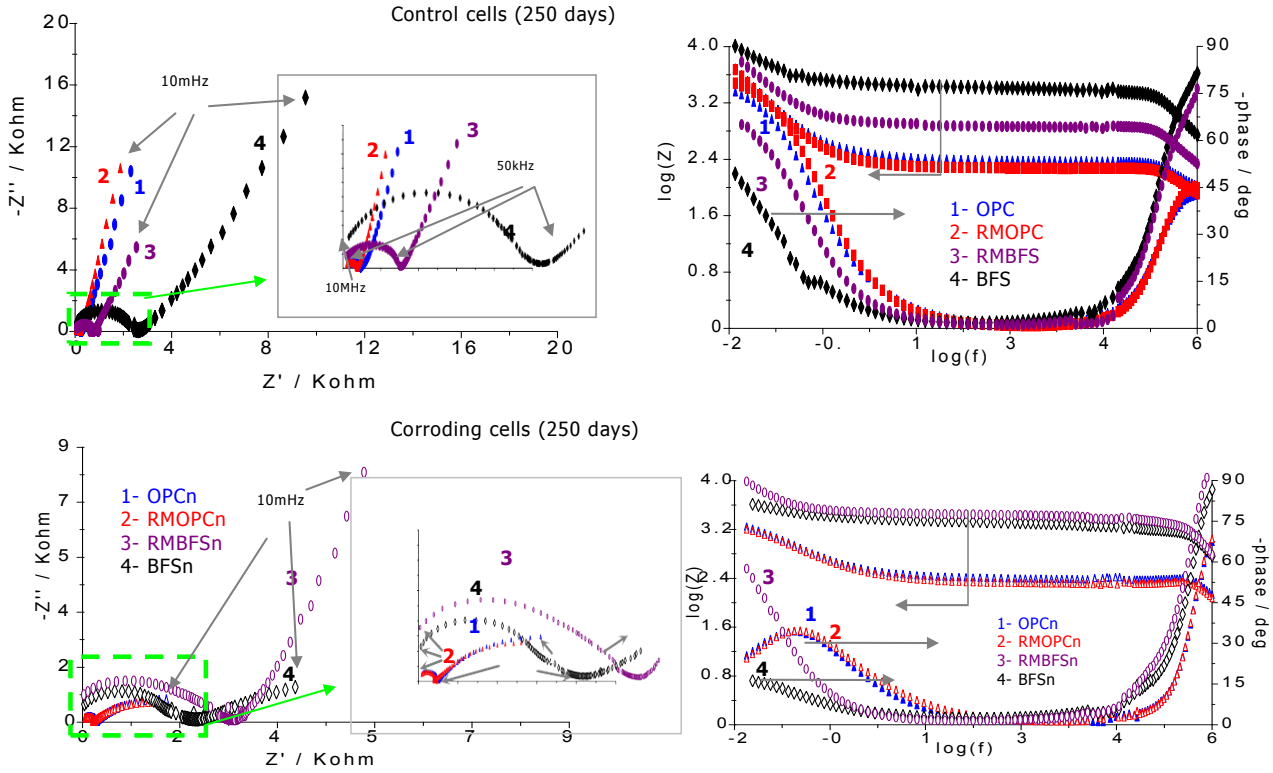

Fig.2 EIS response for control (top) and corroding (bottom) cells after 350 days of conditioning (zoomed areas in the Nyquist plots give the high frequency response, and total response (very low magnitude of |Z|) for corroding cells OPC and RMOPC)

At the stage of 250 days similar EIS response in terms of electrochemical behavior was recorded for all control cells, evidenced by the close to capacitive behavior at low frequencies (indicating situation of passivity). The corrosion resistance for BFS cells is lower, compared to OPC cells (Table 2, R_p values). The influence of RM as BFS replacement is well evident (Table 2, Fig.2, curves 2 and 3, top) and as previously reported for steel in simulated pore solutions of BFS and RM [29,30]. The response for all OPC and BFS specimens differs in the high frequency domain, denoted to the bulk properties of the cement-based matrix in BFS, compared to OPC. The former matrix is generally reported to be denser compared to the latter one [31-35], which gives the difference in bulk matrix resistance, Table 2. Figure 2 (bottom) presents the EIS response for the corroding cells at 250 days, reflecting still passive state for the corroding RMBFSn group and enhanced corrosion activity for the BFSn, OPCn and RMOPCn groups (reduced magnitude of |Z| and phase angle drop to below 40º). The bulk matrix resistance for all specimens (corroding and control groups) increases with time as a result of cement hydration (NaCl slightly influencing the electrical resistivity values), the major difference being denoted to the type of cement i.e. OPC cells (corroding and control) presenting bulk matrix resistance in the range of 400 – 480 Ohm, while for BFS cells, this range is 2126 - 3500 Ohm at 250 days.

Table 2. Best fit parameters EIS response

Control cells

Cell type	R_1	C_1	$R_{p.netw.}$ (R2)	$C_{p.netw.}$ (C2)	$R_{ct.}$ (R3)	C_f (C3)	$R_{red.}$ (R4)	C_{red} (C4)	R_p (R3+R4)	E
	Ohm	nF	Ohm	µF	Ohm.cm^2	µF/cm^2	Ohm.cm^2	µF/cm^2	Ohm.cm^2	mV SCE
OPC	230	2.3	170	350	127	26	2192	20	2300	-183
RMOPC	190	2.5	192	420	165	23	2846	17	3100	-170
BFS	2600	0.3	900	63	312	15	923	23	1200	-65
RMBFS	1090	0.6	1050	102	335	14	1719	15	1700	-120

Corroding cells

Cell type	R_1	C_1	$R_{p.netw.}$ (R2)	$C_{p.netw.}$ (C2)	$R_{ct.}$ (R3)	C_f (C3)	$R_{red.}$ (R4)	C_{red} (C4)	Q_{red}, $Y_0\times10^{-3}$	R_p (R3+R4)	E
	Ohm	nF	Ohm	µF	Ohm.cm^2	µF/cm^2	Ohm.cm^2	µF/cm^2	$\Omega^{-1}s^n$	Ohm.cm^2	mV SCE
OPCn	285	0.7	206	429	37	628	123	1.67, n=0.65		150	-470
RMOPCn	252	0.8	246	140	41	1125	115	1.69, n=0.62		160	-540
BFSn	1770	0.3	356	0.2	22	88	69	0.73, n=0.61		90	-480
RMBFSn	2630	0.2	430	0.1	79	30	1615	15		1700	-130

The charge transfer resistance (R_{ct}) decreased for all corroding cells, compared to the control ones, the specimens RMBFSn, however, behave as control ones (E_{ocp}=-130 mV), exhibiting R_p values in the range of the control cells (1.7 kOhm.cm2), capacitive behavior and higher phase angle (Table 2, Fig.2, specimen RMBFSn). As evident from the electrochemical measurements, 20% red mud as cement replacement, particularly for the BFS cells, results in a corrosion delay in the very aggressive environment of 10% NaCl. The presence of RM in reinforced mortar (and concrete respectively) will account for an increased corrosion resistance in the wastes-modified systems. In order to clarify the responsible mechanisms and related phenomena, microstructural analysis of the bulk cementitious matrix is performed and discussed in what follows.

3.2. Bulk matrix properties (microstructural parameters)

The electrolytic path in reinforced cementitious systems is dependent on the kinetics of ion transport mechanisms. These mechanisms, in addition to the cement hydration and the morphological alterations, are affected by the pore size distribution and the pore connectivity of the bulk concrete material. The critical pore size can be conceived as the diameter of the pore that completes the first interconnected pore pathway in a network, developed by a procedure of sequentially adding pores of diminishing size to this network. The critical pore size lc is a unique transport length scale of major significance for permeability properties and can be associated with the inflection point of the cumulative pore size distribution curve (Fig.3).

Relevant to morphological aspects of the pore structure and ion transport, the pore interconnectivity (defined as the fraction of connected pores out of the total pore area) is used in terms of pore distribution density (PDD). For more details on the fundamental aspects and image analysis of cement-based materials, including mortar, plain concrete and reinforced concrete, please see [16-18].

A set of SEM images on polished sections were made and were further subject to image analysis. The hereby discussed porosity and pore size distribution refer to the bulk matrix only. The structural parameters were averaged from at least 35 locations in the bulk matrix (sample of 2x2 cm). The final data were considered after performing a statistical evaluation in terms of frequency of occurrence (% distribution) vs class (porosity in %). The calculated pore size distribution and

critical pore size are presented in Fig.3bottom) for the bulk matrix (> 250 µm away from the steel surface). Lower porosity was observed for the corroding cells, compared to the control cells, Fig.3 top (as a result from the influence of NaCl as accelerator of cement hydration at initial stages). Further, the influence of BFS and RM is well visible, the lowest recorded porosity being in the RM containing BFS cells. The critical pore size for all investigated groups is similar (approximately 0.634 µm), except for the control BFS cells (0.951 µm).

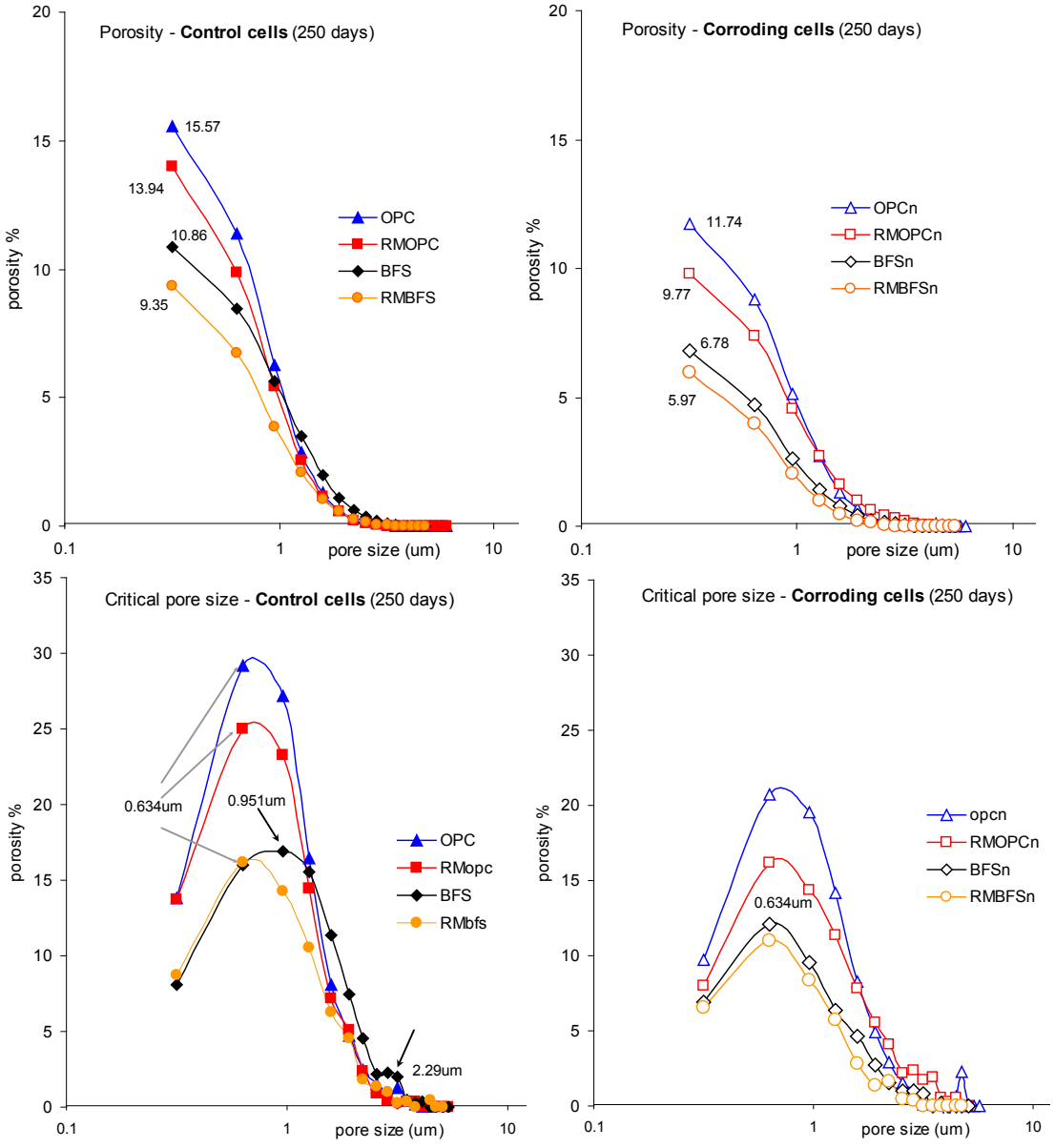

Fig.3 Porosity and pore size distribution (bulk matrix) for control cells and corroding cells

For the BFS control cells, carbonation of the mortar cover was specifically relevant (well known is the high susceptibility of BFS to carbonation), resulting in

coarser structure of the mortar cover, higher pore network connectivity and therefore influence on critical pore size. Additionally, the difference in mortar cover porosity (not hereby presented) and internal bulk matrix porosity and connectivity respectively, for the BFS specimens, resulted in some discrepancies in the correlation of EIS and structural parameters.

The microstructural investigation reveals that the RMBFSn corroding specimens, which electrochemically behave as control ones (i.e. higher corrosion resistance compared to OPCn, BFSn and RMOPCn) exhibit the lowest porosity. In addition to the specific properties of RM in terms of inducing steel passivity, the combination of RM and BFS apparently exerts a significant positive effect (reduced permeability, increased chloride binding mechanisms) and thus is responsible for the observed higher corrosion resistance in these specimens.

Porosity alone is, however, not a factor solely determining the significantly different electrochemical behavior. What has to be considered is the pore interconnectivity in the cement-based matrix and thus the matrix permeability. What will be further discussed is the correlation of these microstructural parameters with derived EIS parameters for the bulk matrix.

A correlation can be made between pore network parameters (Fig.3) and electrochemical (EIS) parameters (Table 2), mainly pore network capacitance ($C_{p.netw}$) and pore network resistance, $R_{p.netw}$ – Fig.4. The higher porosity (P%) and permeability (m/s) in OPC control and corroding cells (Fig.4. bottom right) corresponds to the highest $C_{p.netw}$ and lowest $R_{p.netw}$, the values being lower for OPC corroding cells, compared to OPC control cells (Fig.4 top left). The lowest $C_{p.netw}$ (Fig.4top) corresponds to the lowest permeability values, derived for specimens BFS (both corroding and control groups). The result is very well in line with the derived global bulk electrical resistivity of the matrix in BFS as well (Table 2). Consequently, the BFS matrix (and especially in the presence of RM) in the corroding specimens would be characterized with a larger pore surface area but also increased portion of disconnected and isolated conductive pore pathways (increased pore network resistance). The capacitance values for BFS corroding cells are significantly lower than those for the OPC corroding cells, therefore a comparison of pore network permeability and interconnectivity between OPC and BFS specimens can be reliably derived on the basis of pore network capacitance and resistance.

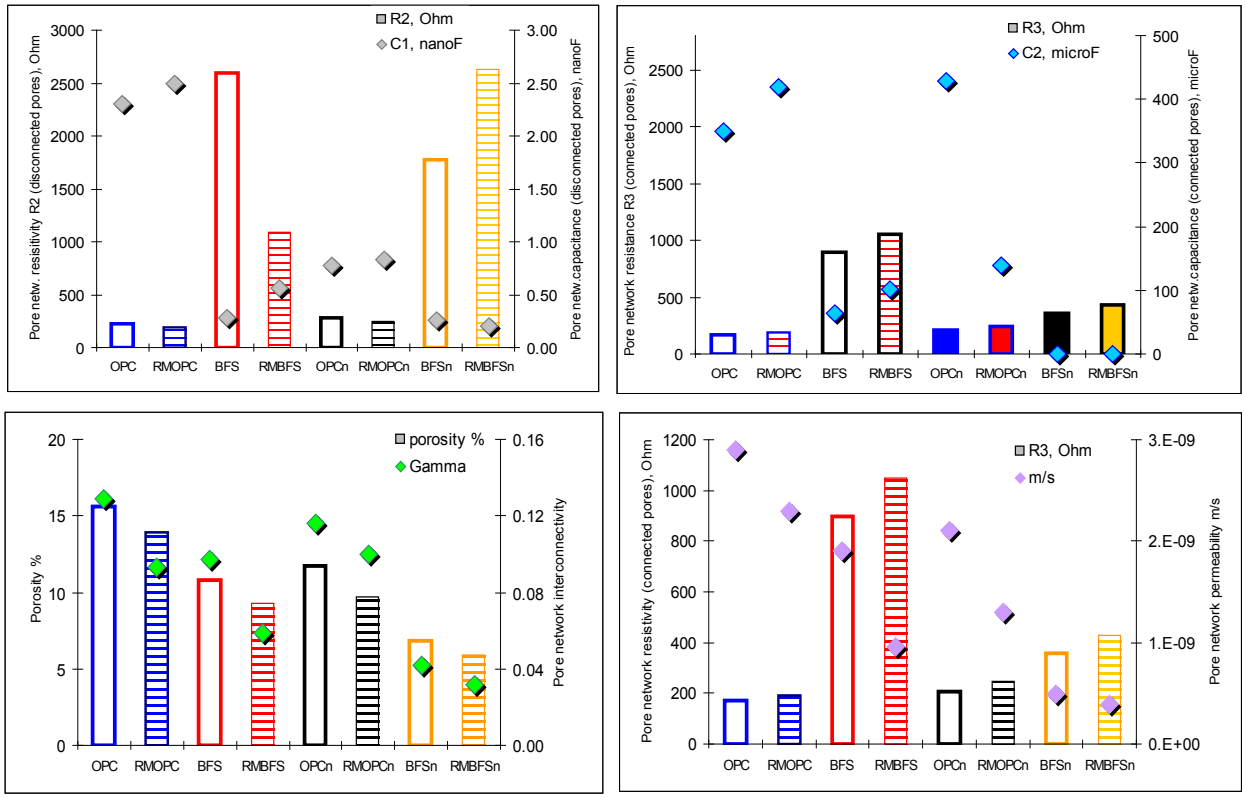

Fig.4 Correlation of pore network capacitance and resistance (top) for disconnected (left) and connected (right) pore pathways; correlation of porosity and pore connectivity (bottom, left) and pore network resistance (connected pores) and permeability (m/s) – (bottom, right)

Consequently (and moreover, after verification with microstructural analysis), it can be stated that EIS is a powerful, non-destructive technique for evaluation of pore network parameters. Combined with the electrochemical parameters, derived for the embedded steel, EIS allows a thorough evaluation of a reinforced concrete system.

4. CONCLUSIONS

Summarizing, this study discussed the corrosion behavior of reinforcing steel in OPC and BFS concrete with and without Red Mud replacement, subjected to chloride-induced corrosion (5% NaCl), in comparison with control cases for both concrete types. Additionally, the electrochemical parameters for the embedded steel were correlated with the microstructural parameters and properties of the bulk concrete matrix. After 250 days of conditioning, corrosion resistance is higher in the RM containing BFS corroding cells, whereas active behavior was observed for the Red mud free corroding cells and the RM containing OPC cells. The higher corrosion

resistance in RMBFS reinforced mortar is denoted to decreased pore-network interconnectivity, evident from the significantly lower pore network capacitance and higher pore network resistance, as derived from EIS and verified on the basis of microstructural analysis. In that sense EIS appears to be a valuable tool for non-destructive and thorough evaluation of not only the electrochemical behavior of reinforcing steel, but also for detailed investigation of the bulk cement based matrix.

5. REFERENCES

1. F. Kehagia, A successful pilot project demonstrating the re-use potential of bauxite residue in embankment construction, Resources, Conservation and Recycling, 54 (2010) 417.
2. M. I. Collazo, M. Izquierdo, X.R. Novoa, C. Perez, Surface treatment of carbon steel substrates to prevent cathodic delamination, Electrochim. Acta, 52 (2007) 7513.
3. A. Anshul, S.S. Amritphale, N. Chandra, N. Ramakrishnan, A. Shrivastava and U.S.P. Verma, Chemically formulated ceramic gamma ray irradiation shielding materials utilising red mud, Advances in Applied Ceramics, 108 (2009) 429.
4. S.S. Amritphale, A. Anshul, N. Chandra, N. Ramakrishnan, A novel process for making radiopaque materials using bauxite—Red mud, Journal of the European Ceramic Society 27 (2007) 1945.
5. Y. Cengeloglu, A. Tor, G. Arslan, M. Ersoz, S. Gezgin, Removal of boron from aqueous solution by using neutralized red mud, Journal of Hazardous Materials, 2007; 142, 412.
6. Y. Liu, Ch. Lin, Y. Wu, Characterization of red mud derived from a combined Bayer Process and bauxite calcination method, Journal of Hazardous Materials, 146 (2007) 255.
7. P.E. Tsakiridis, S. Agatzini-Leonardou, P. Oustadakis, Red mud addition in the raw meal for the production of Portland cement clinker Journal of Hazardous Materials, 116 (2004)103.
8. P.K. Mehta In: Malhotra VM, ed. Pozzolanic and cementitious by products as mineral admixtures for concrete – a critical review, vol. 1. ACI SP-79; 1983, 1.

9. P.K. Mehta In: Malhotra VM, ed. Pozzolanic and cementitious by products in concretes – another look, vol. 1. ACI SP-114; 1989, 1.
10. D.A. Koleva, K. van Breugel, J.M.C. Mol, J.H.W. de Wit, Monitoring chloride-induced corrosion in portland cement and blast furnace slag cement reinforced concrete. In s.n. (Ed.), Corrosion form the nanoscale to the plant (pp. 1-12). Nice: Eurocorr 2009.
11. C. Dehghanian, M. Arjemandi, Cem. Concr. Res. 27 (1997) 937.
12. P. Dinakar, K.G. Babu, Santhanam, Cem. Concr. Comp. 29 (2007)136.
13. O. Çopuroğlu, A.L.A. Fraaij, J.M.J.M. Bijen, Cem. Concr. Res. 36 (2006)1475.
14. D.A. Koleva, J.H.W. de Wit, K. van van Breugel, E. van Westing, J. Electrochem. Soc., 154 (2007) P52.
15. D.A. Koleva, J. Hu, A.L.A. Fraaij, K. van Breugel, J.H.W. de Wit, Cem. Concr. Res., 37 (2007) 604.
16. J. Serra, Image analysis and mathematical morphology. London: Academic Press, 1982.
17. G. Ye, Experimental Study and Numerical Simulation of the Development of the Microstructure and Permeability of Cementitious Materials, PhD thesis, Delft University of Technology, Delft, 2003.
18. J. Hu, P. Stroeven, Image Analysis Stereology, 22 (2003) 97.
19. D.A. Koleva, Z. Guo, K. van Breugel, J.H.W. de Wit, Mater. & Corrosion, 61 (2010) 561.
20. D.A. Koleva, (2007) Corrosion and Cathodic Protection in Reinforced concrete, PhD Thesis, Delft University of Technology, Delft.
21. A.A. Sagüés, S.C. Kranc, E.I. Moreno, Corr. Sci., 37 (1995)1097.
22. V. Feliú, J.A. González and S. Feliú, J. Electrochem. Soc., 151 (2004) B134.
23. D.A. Koleva, Z. Guo, K. van Breugel, J.H.W. de Wit, Mater. Corrosion, 60 (2009) 344.
24. M. Cabeza, P. Merino, A. Mirandab, X.R. Novoa, I. Sanchez, Cem Concr Res., 32 (2002)881.
25. M.F. Montemor, M.P. Cunha, M.G. Ferreira, A.M. Simões, Cem. Concr. Comp., 24 (2002) 45.
26. V. Feliú, J.A. González, C. Andrade, S. Feliú, Corr. Sci., 40 (1998) 975.
27. F. Wenger, J. Galland, Electrochim. Acta, 35 (1990)1573.
28. L. Fedrizzi, F. Azzolini, P. L. Bonora, Cem. Concr. Res., 35 (2005) 551.
29. D.A. Koleva, The significant delay of chloride-induced corrosion in reinforced mortar, containing red mud as cement replacement, Submitted to J. Electrochem. Soc. 2011.

30. D.A. Koleva, Jie Hu, K. van Breugel, J. H. W. de Wit, J. M. C. Mol, Steel corrosion resistance in model solutions, containing wastes, The European Corrosion Congress: EUROCORR 2010, Sept 13th – 17th, Moscow, proceedings CD; EFC event 324, Publisher: Dechema e.V. (2010)
31. A. Bouikni, R.N. Swamy, A. Bali, Constr. Build. Mater., 2009; 23, 2836.
32. O.E. Giorv, O. Vennesland, Cem. Concr. Res., 1979; 9, 229.
33. D. Manmohan, P.K. Mehta, Cem. Concr. Aggr.,1981; 3, 63.
34. A.D.M. Kumar In: Proc. 8th Conf. Chemistry of Cement, Brazil, 1986; 73.
35. R.D. Hooton In: Frohnsdorff G, ed. Blended cement, ASTM STP 897; 1986, 128.